INTERNATIONAL JOURNAL OF
ENERGY AND ENVIRONMENT

Volume 9, Issue 6, 2018 pp.591-606
Journal homepage: www.IJEE.IEEFoundation.org

Dynamic behavior of cracked functionally graded (FG) material pipe conveying fluid

Talib EH. Elaikh, Sadiq M. Hmod, Eman R. Bustan

Department of Mechanical Engineer, College of Engineering, Thi-Qar University, Iraq.

Received 29 Sep. 2018; Received in revised form 21 Oct. 2018; Accepted 27 Oct. 2018; Available online 1 Nov. 2018

Abstract
Dynamic behavior of cracked functionally graded (FG) pipe conveying fluid lying on visco-elastic foundation is investigated in this paper. The crack is demonstrated as a massless torsional spring. The properties of the material are changed constantly across the micro-pipes thickness and depend on power law distribution. Efficient numerical procedure by Galerkin's method is developed to find the natural frequencies and stability for cracked FG pipe. The effects of cracks location, depth of crack, gradient index, and foundation parameters in FG pipes conveying fluid with certain flow velocity on frequencies are investigated. The present method is carefully checked by comparing their results for cracked pipe conveying fluid with the available results in literature. From the comparison, a reasonable agreement was found (i.e. the maximum discrepancy percentage was 1.5%). The results indicated that the fundamental natural frequency decreased due to the crack presents. Also, the flow velocity for FG pipe increased with gradient index increasing.

Keywords: Fluid-conveying FG pipe; Open edge crack; Galerkin's method; Visco-elastic foundation.

1. Introduction
The dynamic behavior of pipe convey fluid have been widely range of palliations due to its extensive in different application such as industries, petroleum, chemical, aerospace, gasoline transportation systems, biological engineering systems, heat exchanger, and Nano-fluidic devices [1]. These pipes are subjected to various damages during their service life, such as corrosion, internal pressure, and fatigue. Therefore, the investigation into the presence of a crack in the pipeline is important, especially if the pipeline carries oil or petrochemical fluids. When a crack is present in a structure, changes in the vibrational frequencies occurs as a result of this cracking. Therefore, the dynamic behavior of cracked pipe containing fluid has been studied by researchers in past decades.
Crack detection in fluid-conveying pipes utilizing a vibration-based approach was presented by Mahjoob, M. et al [2] with the FIM and experiments approach. Crack is modeled by some rigidity reduction in the element incorporating the crack. With this modeling approach, the crack position can be related to changes in natural frequencies through a straightforward relation. Son, I. S, et al. [3] proposed the numerical method for studying the dynamic stability of a rotating (clamped-free) pipe convey fluid with a crack and tip mass. The results presented that the critical fluid velocity is reduced when the tip mass is increased. Kwan et al. [4] studied the effect of attached mass and crack on the dynamic stability of an elastically restrained fluid-

conveying pipe. They studied the critical flow velocity for the flutter and divergence due to the variance in the position and stiffness of supported spring. The results for crack severity increases, the critical flow velocity becomes larger when the spring position existed in the center of the pipe. Sheng et al. [5] investigated the vibration stability of fluid-conveying pipe with crack and lying on an elastic foundation subjected to the follower force. The effects of elastic foundation stiffness, follower force, and crack location on the stability of the pipes were analyzed. Results showed that the stiffness of the elastic foundation can perform the pipes stability effectively. Eslami et al [6] studied the effect of crack location and depth of the crack on vibration behavior of pipe conveying fluid with clamped at both ends. The results showed that increased crack depth improves flexibility, so the local stiffness reduced the location of crack. This leads to a reduction of both vibration frequency and critical fluid flow of the pipe with crack. Muhsin et al. [7] suggested experimental and numerical techniques to study the effect of cracks on the vibration frequency of fluid -conveying pipe with simply supported end conditions. Crack depth was investigated with different flow velocity values. They were found that the natural frequency of the pipes decreases when the crack depth is increased. Furthermore, the mechanical behavior of FGM structure has been excessively studied by researchers in past decades. But the literature related to the dynamics of fluid-conveying FGM pipes are few. Sheng and Wang [8] investigated the effect of axial and thermal loads on vibration behavior of flowing fluid FG cylindrical shells embedded in elastic medium. From the result, it can be seen that the natural frequency of FGM cylindrical shell conveying fluid was decreased as the temperature variation between the inner surface and the outer surface and the axial load's increase. Effect of axial load and temperature field on the stability of fluid-conveying cantilever FGM pipes was investigated by Hosseini, M and Falahzadeh, S. A. [9] using extended Galerkin's method. Liang et al [10] demonstrated the in-plane free vibration frequency of the fluid-conveying FG curved pipes. Complex mode method was used to study the first four vibration frequencies. Generalized the integral transformation technique was used to discuss the dynamic behavior of axially FG pipes with flowing fluid by ZHU, C. G, and Si-Peng X. U [11].
Dynamic behaviors of fluid- conveying FG pipe with multi-span using the DSM was investigated by Deng et al. [12]. Nonlinear vibration and post-buckling of a fluid-conveying FG pipe were studied by Tang, et al. [13]. They found that nonlinear frequency increased with initial amplitude, but decreased with flow velocity.
Through the above literature, the dynamic behavior of fluid-conveying FGM pipe with crack has not been studied. Therefore, dynamic behavior for fluid-conveying FG pipe lying on a viscoelastic foundation with open edge crack is investigated in this paper. The governing equation is derived by using energy Hamilton's principle with Euler-Bernoulli model. Galerkin's method is developed to find the vibration frequencies and stability of the cracked FG fluid conveying pipe for simply supported end conditions. The results computed by Galerkin's method are compared with those in a published literature to verify the current method. The effects of different parameters like as a crack depth and location, viscoelastic foundation parameter, volume fraction n, and dimensionless flow velocity on the stability and free vibration of cracked FGM pipes conveying fluid are discussed.

2. Mathematical formulation

Figure 1 explains the schematic of the fluid-conveying FG pipe resting on a visco-elastic foundation with crack presence. L is the length of pipe, u refers to flow velocity x_c is crack location. θ, and $2b$ are the half-angle of the total crack depth (the crack severity will be indicated by $(\alpha = \theta_c / \pi)$ as percentage) and the length of a crack, respectively. Do is outside diameter, Di inside diameter, a/h is size of crack, and α is the angle between the centerline.
The effective material properties are given by [14]:

$$F(n) = (F_o - F_i)\left(\frac{2n+h}{2h}\right)^k + F_i \tag{1}$$

$$E(n) = (E_o - E_i)\left(\frac{2n+h}{2h}\right)^k + E_i \tag{2}$$

$$\rho(n) = (\rho_o - \rho_i)\left(\frac{2n+h}{2h}\right)^k + \rho_i \tag{3}$$

where (k) is the normal coordinate across the wall thickness (−h/2 ≤ k ≤h/2), $E(k)$ and $\rho(k)$ is the effective modulus of elasticity, the effective density, respectively and (ν) is the Poisson's ratio which is considered constant.

In order to find the frequency equation for cracked pipe, firstly the pipe is divided in two segments at cracked section. The crack unit is simulated as shown in (Figure 2) as a spring twist that connects un-cracked FG pipe sections on both sides.

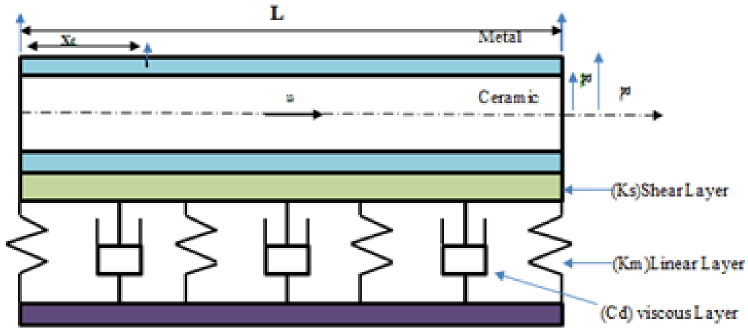

(a)

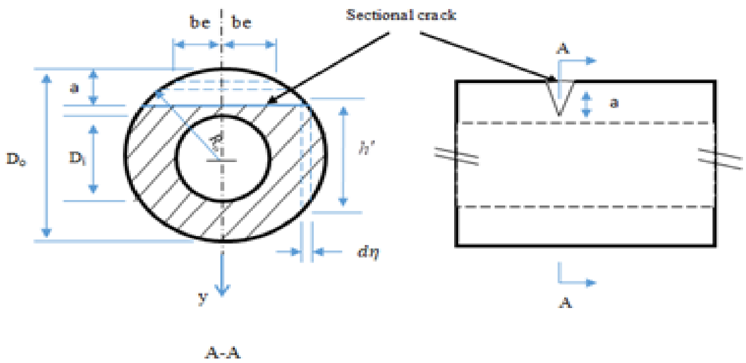

(b)

Figure 1. (a) Schematic diagram of FG pipe conveying fluid lying visco-elastic foundation with crack; (b) Circular hollow cross-section of the cracked section.

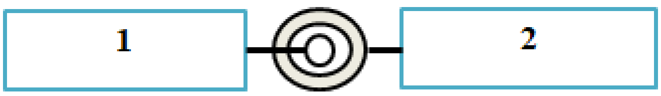

Figure 2. Model of crack of FGM pipe and Rotational spring model.

And, then, the vibration equation is derived using energy principle and the variation approach. To this end, the kinetic energy of the internal fluid flow T_f is expressed as follows:

$$T_f = \frac{1}{2} m_f \left[\int_0^{x_c} V_f^2 + 2V_f \frac{\partial^2 w_1}{\partial x \partial t} + \left(\frac{\partial w_1}{\partial t}\right)^2 + \int_{x_c}^{L} \left(\left(\frac{\partial w_2}{\partial t}\right)^2 + 2V_f \frac{\partial^2 w_2}{\partial x \partial t} + V_f^2 \right) \right] dx \tag{4}$$

where m_f is represented the mass density for fluid, and

$$m_f = \rho_f A_f \tag{5}$$

The kinetic energy for the cracked FG pipe conveying fluid can be expressions as

$$T_p = \frac{1}{2} m_p \left[\int_0^{x_c} \left(\frac{\partial w_1}{\partial t} \right)^2 dx + \int_{x_c}^{L} \left(\frac{\partial w_2}{\partial t} \right)^2 dx \right] \tag{6}$$

where m_p is represented the effective mass of pipe, and can be written as

$$m_p = \int_0^{2\pi R_m} \int_{-h/2}^{h/2} \rho(n) \frac{R_m + n}{R_m} dsdn = \int_0^{2\pi R_m} \int_{-h/2}^{h/2} \left[(\rho_c - \rho_m) \left(\frac{2n+h}{2h} \right)^k + \rho_m \right] \left(1 + \frac{n}{R_m} \right) dnds = m^* \rho_k \tag{7}$$

And

$$m^* = 2\pi R_m h \rho_m, \rho_k = \frac{1 + \rho_R k}{k+1} + h_R (1 - \rho_R) \left(\frac{1}{k+1} - \frac{1}{2(k+1)} \right), \rho_R = \frac{\rho_c}{\rho_m}, , , , h_R = \frac{h}{R_m}, , , , E_R = \frac{E_c}{E_m} \tag{8}$$

To drive the expression of strain energy, assuming that the pipeline is elastic, and the stress – strain relation is given by:

$$\sigma_x = \frac{E(n)}{1 - \nu^2} \varepsilon_x \tag{9}$$

The transverse displacements along $u_{(x,t)}$ is written as follows

$$u_{(x,t)} = -y \frac{\partial w}{\partial x} = -\left(Y(s) - n \frac{dZ}{ds} \right) \frac{\partial w}{\partial x} \tag{10}$$

The axial strain for small deformation assumption is written as:

$$\varepsilon_x = \frac{\partial u_x}{\partial x} = -\left(Y(s) - n \frac{dZ}{ds} \right) \frac{\partial^2 w}{\partial x^2} \tag{11}$$

Then, the expression of strain energy for FG pipe is obtained as:

$$U_s = \frac{1}{2} \int_0^{x_c} \int_{-h/2}^{h/2} \int_0^{2\pi} \sigma_x \varepsilon_x (R_m + n) d\theta dn dx + \frac{1}{2} \int_{x_c}^{L} \int_{-h/2}^{h/2} \int_0^{2\pi} \sigma_x \varepsilon_x (R_m + n) d\theta dn dx \tag{12}$$

Or,

$$U_s = \frac{1}{2} \int_0^{x_c} \int_{-h/2}^{h/2} \int_0^{2\pi Rm} \sigma_x \varepsilon_x \left(\frac{R_m + n}{R_m} \right) dsdndx + \frac{1}{2} \int_{x_c}^{L} \int_{-h/2}^{h/2} \int_0^{2\pi Rm} \sigma_x \varepsilon_x \left(\frac{R_m + n}{R_m} \right) dsdndx \tag{13}$$

Now, substituting Eqs (9) and (11) into equation (13), and perform some manipulation, the bending strain energy is expressed in terms of pipe deflection as follows:

$$U_s = \frac{1}{2}\alpha\left[\int_0^{x_c}\left(\frac{\partial^2 w_1}{\partial x^2}\right)^2 + \int_{x_c}^{L}\left(\frac{\partial^2 w_2}{\partial x^2}\right)^2\right]dx \tag{14}$$

where α is the flexural stiffness for FGM pipes, and it can be written as:

$$\alpha = \alpha' J_k ,\ \alpha' = \frac{\left(1+0.25{h_R}^2\right)\pi E_m R_m^3 h}{1-v^2} \tag{15}$$

And

$$J_k = \frac{1}{1+0.25{h_R}^2}\left[\begin{array}{l}\frac{1+E_R k}{k+1} + 3(1-E_R)h_R\left(\frac{1}{k+2}+\frac{1}{2(k+1)}\right) + 3(1-E_R)h_R\left(\frac{1}{k+3}+\frac{1}{k+2}+\frac{1}{4(k+1)}\right) + \frac{1}{4}E_R h_R \\ +3(1-E_R){h_R}^2\left(\frac{1}{k+4}+\frac{1}{2(k+3)}+\frac{1}{4(k+2)}+\frac{1}{8(k+1)}\right)\end{array}\right] \tag{16}$$

The virtual work done by the external transverse forces F^{ext} exerted on the cracked FG pipe by the visco-elastic foundation can be calculated as:

$$W^{ext} = \left[\int_0^{x_c}\left[K_s\frac{\partial^2 w_1}{\partial x^2} - C_d\frac{\partial w_1}{\partial t} - K_m w_1\right]dx + \int_{x_c}^{L}\left[K_s\frac{\partial^2 w_2}{\partial x^2} - C_d\frac{\partial w_2}{\partial t} - K_m w_2\right]dx\right] \tag{17}$$

The dynamic version of a virtual displacements principle's or Hamilton’s principle is

$$\int_{t_1}^{t_2}\left[\left(\delta U_s - \delta W^{ext}\right) - \delta T\right]dt = 0 \tag{18}$$

Substituting Eqs (6), (14), and (17) into equation (18), integrating by parts and presenting the coefficients of (δw) zero, leads to the vibration equations for two segment of cracked FG pipe as follows:

$0 \le x \le x_c$

$$\alpha\frac{\partial^4 w_1}{\partial x^4} + \left[\rho V_f^2 - K_S\right]\frac{\partial^2 w_1}{\partial x^2} + 2V_f\sqrt{\rho}\frac{\partial^2 w_1}{\partial x \partial t} + \left[m_p + \rho\right]\frac{\partial^2 w_1}{\partial t^2} + C_d\frac{\partial w_1}{\partial t} + K_M w_1 = 0 \tag{19a}$$

$x_c \le x \le L$

$$\alpha\frac{\partial^4 w_2}{\partial x^4} + \left[\rho V_f^2 - K_S\right]\frac{\partial^2 w_2}{\partial x^2} + 2V_f\sqrt{\rho}\frac{\partial^2 w_2}{\partial x \partial t} + \left[m_p + \rho\right]\frac{\partial^2 w_2}{\partial t^2} + C_d\frac{\partial w_2}{\partial t} + K_M w_2 = 0 \tag{19b}$$

The vibration equations of motion for cracked FG pipe convey fluid in terms of dimensionless form may be written as:

$0 \le \eta \le \eta_c$

$$J_k\frac{\partial^4 W_1}{\partial \eta^4} + \left[u^2 - K_S\right]\frac{\partial^2 W_1}{\partial \eta^2} + 2u\beta^{\frac{1}{2}}\frac{\partial^2 W_1}{\partial \eta \partial \tau} + \left[\beta + (1-\beta)\rho_k\right]\frac{\partial^2 W_1}{\partial \tau^2} + C_d\frac{\partial W_1}{\partial \tau} + K_M W_1 = 0 \tag{20a}$$

$\eta_c \le \eta \le 1$

$$J_k\frac{\partial^4 W_2}{\partial \eta^4} + \left[u^2 - K_S\right]\frac{\partial^2 W_2}{\partial \eta^2} + 2u\beta^{\frac{1}{2}}\frac{\partial^2 W_2}{\partial \eta \partial \tau} + \left[\beta + (1-\beta)\rho_k\right]\frac{\partial^2 W_2}{\partial \tau^2} + C_d\frac{\partial W_2}{\partial \tau} + K_M W_2 = 0 \tag{20-b}$$

And, the non-dimensional form of FG cracked pipe is given as:

$$x \to \frac{\eta}{L},, w \to \frac{W}{L},, \eta_c \to \frac{x_c}{L} \tau \to \frac{t}{L^2}\left(\frac{\alpha'}{\rho + m^*}\right),, c = \frac{EIC}{L}, u \to V_f L \sqrt{\frac{\rho}{\alpha'}},, \beta \to \frac{\rho}{\rho + m^*}$$
$$K_M \to \frac{L^4}{\alpha'} K_m,, k_s \to \frac{L^2}{\alpha'} K_S,, C \to \frac{C_d L^2}{\sqrt{\alpha'(\rho + \alpha')}} \tag{21}$$

3. Crack modeling

The additive strain energy produced by the crack can be represented as a flexibility coefficient expressed by the stress intensity factor, which can be obtained by the Castiglione theory. Therefore, the crack local flexibility is defined by [15].

$$C_{ij} = \frac{\partial u_{ij}}{\partial P_j} = \frac{\partial^2}{\partial P_i \partial P_j}\left(\int_{-be}^{be}\int_0^a J d\eta d\varsigma\right) \tag{22}$$

where P_i, P_j and u_{ij} are the load and a local additional displacement, respectively.
The strain energy function J is [16]:

$$J = \frac{1}{E(k)}(K_I)^2 \tag{23}$$

The local flexibility factor is given by

$$C = \frac{\partial}{\partial M}\int_0^a \int_{-be}^{be} \frac{K_I^2}{E(n)} d\eta d\varsigma \tag{24}$$

where (be) can be written as:

$$be = \sqrt{\frac{D_o^2}{4} - \left(\frac{D_o}{2} - \varsigma\right)^2} \tag{25}$$

And (K_I) is a stress of intensity factors for bending is given by

$$K_I = \frac{Mh'}{2I}\sqrt{\pi\varsigma' F(\eta)} \tag{26}$$

The function $F(\eta)$ is given by [17]

$$F(\eta) = \sqrt{\frac{\tan(\pi\eta/2)}{(\pi\eta/2)}\left[\frac{0.923 + 0.199(1 - \sin(\pi\eta/2))^4}{\cos(\pi\eta/2)}\right]} \tag{27}$$

For an FGM pipe with an open edge crack under bending, the analytical solution for equivalent rotational spring stiffness K_t is related to the flexibility C by [18].

$$K_t = \frac{1}{C} \tag{28}$$

where C is local flexibility of crack and can be written as [17]

$$C = \frac{1028h^2R}{\pi E' D_o^6 (1-d^4)^2} \int_o^\theta \cos^4 \alpha d\alpha \int_0^{a/h} xF^2(\eta) d\eta \tag{29}$$

Where $R = \frac{D_o(1+d)}{4}; h = \frac{D_o(1-d)}{2}; E' = \frac{E(n)}{(1-v^2)}; d = \frac{D_i}{D_o}; I = \frac{\pi}{64}\left(D_o^4 - D_i^4\right)$

and, the local flexibility of crack in non-dimensional form is:

$$c = \frac{64(1+d)(1-d)^2}{\pi(1-d^4)^2} \int_o^\theta \cos^4 \alpha d\alpha \int_0^{a/h} \eta F^2(\eta) d\eta \tag{30}$$

4. Mode shape assumption

The mode shape function of the cracked FG pipe can be expressed as the sum of the formation function of the un-cracked FG pipe and the polynomial of x, expressed as follows [19].

$$(0 \le x \le x_c)$$
$$\phi_{i1}(x) = \bar{\phi}(x) + A_o + A_1 x + A_2 x^2 + A_3 x^3, \tag{31a}$$

$$(x_c \le x \le L)$$
$$\phi_{i2}(x) = \bar{\phi}(x) + B_o + B_1 x + B_2 x^2 + B_3 x^3, \tag{31b}$$

The eight constants A_n and B_n (n = 0, 1, 2, 3) in the above formulas (31) can be acquired by applying both the end conditions for pinned FG pipe and the compatibility conditions at the crack position.
The derivatives of *Eqs* (31a) and (31b) are:

$$\phi_1'(x) = \bar{\phi}'(x) + A_1 + 2A_2 x + 3A_3 x^2, \phi_1''(x) = \bar{\phi}''(x) + 2A_2 + 6A_3 x, \phi_1'''(x) = \bar{\phi}'''(x) + 6A_3 \tag{32}$$

$$\phi_2'(x) = \bar{\phi}'(x) + B_1 + 2B_2 x + 3B_3 x^2, \phi_2''(x) = \bar{\phi}''(x) + 2B_2 + 6B_3 x, \phi_2'''(x) = \bar{\phi}'''(x) + 6B_3 \tag{33}$$

The continuity and compatibility conditions of the cracked FG pipe with Pinned at both ends at $x = x_c$ are:

$$\phi_{i1}(x_c) = \phi_{i2}(x_c), \frac{\partial^2 \phi_{i1}(x_c)}{\partial x^2} = \frac{\partial^2 \phi_{i2}(x_c)}{\partial x^2}, \frac{\partial^3 \phi_{i1}(x_c)}{\partial x^3} = \frac{\partial^3 \phi_{i2}(x_c)}{\partial x^3}$$
$$\left(\frac{\partial \phi_{i2}(x_c)}{\partial x} - \frac{\partial \phi_{i1}(x_c)}{\partial x}\right) = \frac{EIC}{L}\left(\frac{\partial^2 \phi_{i2}(x_c)}{\partial x^2}\right) \tag{34}$$

The boundary conditions of the Pinned – Pinned FG pipe are:

$$\phi_{n1}(0) = \frac{\partial^2 \phi_{n1}(0)}{\partial x^2} = 0, \phi_n(L) = \frac{\partial^2 \phi_{n2}(L)}{\partial^2 x} = 0 \tag{35}$$

Substituting equations (21) and (22) into equations (23) and (24), yields:

$$A_0 == \mathrm{B}_2 = 0, \quad A_1 = -c * \eta_c \pi^2 (1 - 1l\eta_c) \sin \pi\eta_c,$$
$$A_3 = B_3 = 0, B_o = c * \eta_c \pi^2 \sin \pi\eta_c, B_1 = -c * \eta_c \pi^2 \sin \pi\eta_c. \tag{36}$$

And, the standard' mode functions for P-P pipe are;

$$\bar{\phi}(\eta) = \sin(bn\pi\eta), b_n == \pi, 2\pi, ,, \mathrm{n} = 1,2 \tag{37}$$

By coupling the continuity, compatibility and boundary conditions of the P-P FG pipe, the mode shape function it is obtained as:

$$(0 \le \eta \le \eta_c), \phi_{i1}(x) = \sin(i\pi\eta) - (\frac{\eta_c - 1}{\eta_c})\left[\eta_c * c * (i\pi)^2 \sin(i\pi\eta_c)\right]\eta \tag{38a}$$

$$(\eta_c \le \eta \le 1), \phi_{i2}(x) = \sin(i\pi\eta) + (1-\eta) * \eta_c * c * (i\pi)^2 \sin(i\pi\eta_c) \tag{39b}$$

5. Application of Galerkin's method

In order to solve the vibration equation (Eq. (28)), Galerkin's method is applied to discretize the partial differential equation (PDE) to an ordinary differential equation (ODE). By using the Galerkin's method, the lateral displacement function W (x, t) of the FG pipe can be assumed as:

$$W(\eta, \tau) = \sum_{r=1}^{2} \phi_r(\eta) q_r(\tau) \tag{40}$$

where $\phi_r(\eta)$ and $q_r(\tau)$ are the shape functions and the generalized coordinates, respectively. Substituting *Eq*s (40) into equation (20)), yields

$$\sum_{r=1}^{2} \left[J_k \phi_r^{iv} q(\tau) + (u^2 - k_s)\phi_r'' q(\tau) + 2\omega\beta^{0.5} u \phi_r' \dot{q}(\tau) + \left[\beta + (1-\beta)\rho_k\right]\omega^2 \phi_r \ddot{q}(\tau) + C_d \omega \phi_r \dot{q}(\tau) + K_m \phi_r q(\tau)\right] = 0 \tag{41}$$

Multiplying *Eq*s (41) by the boundary residual value function $\phi_s(\eta)$, $(s = 1,2)$ and integrating along the whole span of the pipe and setting the final result to zero, give;

$$M\ddot{q} + C\dot{q} + Kq = 0_{,,,} q = (q_1, q_2)^T, ,(r, s = 1,2) \tag{42}$$

Where the expressions of M, C, and K are respectively

$$M(r,s) = [\beta + (1-\beta)\rho_k] \int_0^1 \phi_r(\eta)\phi_s(\eta) d\eta = [\beta + (1-\beta)\rho_k] \left[\int_0^{\eta_c} [\phi_{1r}(\eta)\phi_{1s}] d\eta + \int_{\eta_c}^{1} [\phi_{2r}(\eta)\phi_{2s}] d\eta\right] \tag{43}$$

$$K = J_k B_1 + (u^2 - k_s) B_2 + K_m \delta_{sr},,, C = 2u\beta^{0.5} B_3 + C_d \delta_{sr} \tag{44}$$

where δ_{sr} is a Kronecker delta ($\int_0^1 \phi_s \phi_r d\eta = \delta_{sr}$), as well as the fact that ($\phi_r^{iv} = \lambda_r^4 \phi_r$) being the r^{th} dimensionless eigenvalue of pipe.

And

$$\phi_r^{iv} = \lambda_r^4 \phi_r,, \delta_{sr} = \int_0^1 \phi_s \phi_r q(\tau) d\eta,,, C_{sr} = \int_0^1 \phi_s \phi_r'' q(\tau) d\eta,,, b_{sr} = \int_0^1 \phi_s \phi_r' \dot{q}(\tau) d\eta \tag{45}$$

$$B_1(r,s) = \int_0^1 \phi_r^{iv}(\eta)\phi_s(\eta) d\eta = \int_0^{\eta_c} [\phi_{1r}^{iv}(\eta)\phi_{1s}] d\eta + \int_{\eta_c}^{1} [\phi_{2r}^{iv}(\eta)\phi_{2s}] d\eta \tag{46}$$

$$B_2(r,s)=\int_0^1 \phi_r''(\eta)\phi_s(\eta)d\eta=\int_0^{\eta_c}[\phi_{1r}''(\eta)\phi_{1s}]d\eta+\int_{\eta_c}^1[\phi_{2r}''(\eta)\phi_{2s}]d\eta \tag{47}$$

$$B_3(r,s)=\int_0^1 \phi_r'(\eta)\phi_s(\eta)d\eta=\int_0^{\eta_c}[\phi_{1r}'(\eta)\phi_{1s}]d\eta+\int_{\eta_c}^1[\phi_{2r}'(\eta)\phi_{2s}]d\eta \tag{48}$$

In order to facilitate the solution of the eigenvalues, the Eqs (42) of the cracked FG pipe is converted into the following form:

$$\overline{M}\dot{X}+\overline{K}X=0 \tag{49}$$

$$\overline{M}=\begin{bmatrix} M & 0\\ 0 & I\end{bmatrix},\ \overline{K}=\begin{bmatrix} C & K\\ -I & 0\end{bmatrix},\ X=\begin{Bmatrix}\dot{d}\\ d\end{Bmatrix} \tag{50}$$

For complex modal analysis, there are:

$$X=e^{\lambda_f \tau}\Theta \tag{51}$$

where λ_f is the complex eigenvalue.
And

$$i=\sqrt{-1},\lambda_f=b_f+w_f i \tag{52}$$

Substituting the *Eq*s (38) into *Eq*s (37) to solve the above eigenvalue problem, the vibration frequency of the cracked FG pipe can be obtained.

6. Results of vibration for cracked FG pipe

The analytical results of the cracked FG pipe conveying fluid using Galerkin's method are investigated. Also, in this section, the effects of crack depth, the crack position, gradient index k and parameter of visco-elastic foundation into the fundamental natural frequency of the FG pipe carrying fluid are discussed.
Firstly, to examine the validity of the obtained results, the problem of a simply supported cracked homogenous pipe without foundation is considered. The frequency ratio for different crack depth and location are considered and comparison between present and with those obtained by Jweeg M. J. e t. [7] for the first mode are given in Table 1, Table 1 shows that the values of the natural frequency ratio agree with the previous ones in [7]. The frequency ratio is defined as:

$$\Omega=\frac{\omega(crackedfrequency)}{\omega_o(uncrackedfrequency)} \tag{53}$$

Table 1. Frequency ratio for different crack depth and location for cracked homogenous pipe.

Crack depth ratio a/h	Crack position $x_c=0.25$		Error%	Crack position $x_c=0.5$		Error%
	Present	Ref.[7]		Present	Ref.[7]	
0.3	0.97324	0.97577	0.26	0.94723	0.95837	1.17
0.5	0.93301	0.94309	1.08	0.90320	0.91303	1.08
0.7	0.91250	0.92358	1.2	0.83254	0.84523	1.5
0.9	0.88923	0.89194	0.3	0.82743	0.83125	0.46

6.1 Effect of the crack depth

Crack depth effect on vibration frequency and frequency ratio for pinned FG pipe with different dimensionless flow velocity and cracks location is presented in this subsection.

The influence of crack depth ratio on dimensionless frequency for the first mode of fundamental eigenvalues for (P-P) end conditions FG pipe with dimensionless fluid velocity are shown in Figure 3. The results are presented for different shear foundation parameter a/h, $a/h = 0.3, 0.5$, and 0.7. $(K_m = 0.01, C_d = 0.01, K_s = 0.01, k = 1)$, is used for numerical computation. The results showed that the first frequency decreases with increasing crack depth.

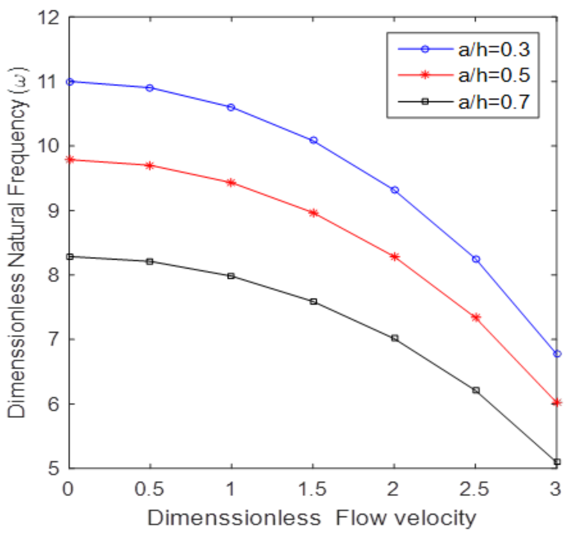

Figure 3. Effect of crack depth (a/h) on the first mode frequency for (P-P) boundary condition.

Figure 4 demonstrates the influence of crack depth ratio a/h on the lowest two mode frequency ratio of the (simply supported) FG pipe conveying flow versus crack location. The results are offered for different crack depth ratio, $a/h = 0.3$, $a/h = 0.5$ and $a/h = 0.7$. In this case, $K_m = 50$, $K_s = 20$, $C_d = 10$ and gradient index $k = 1$. According to Figure 4, the depth of crack tends to decrease the bending stiffness of the FG pipe convey flow. The frequency ratio with curves of crack location is symmetric for geometrically symmetric structures such as hinged-hinged. When the crack is in the midpoint of the pinned-pinned FG pipe, the frequency ratio is minimum.

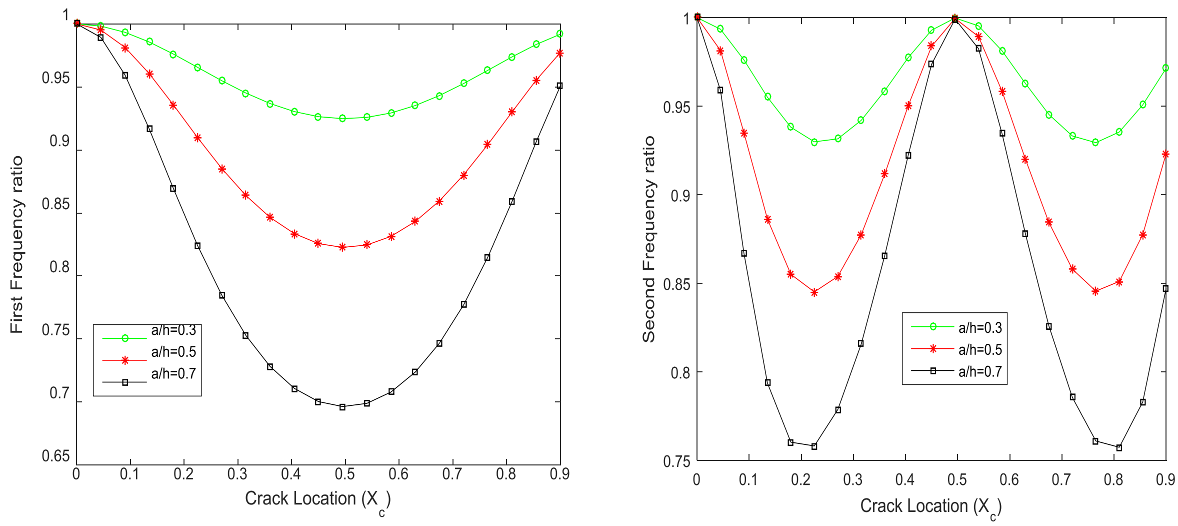

Figure 4. Crack depth (a/h) effect on first two frequency ratio for (P-P) boundary condition.

6.2 Effect of the gradient index (k)

This subsection presents the effect of the gradient index (k) on frequency ratio of simply supported FG pipe with different crack depth ratio. Figure 5 presents the infllunce the gradient index (k) on lowest three frequency ratio for pinned-pinned cracked FGM pipes versus crack depth ratio). Here, the results are presented for different gradient index, k = 1, k = 3 and 5. In this case, $K_m = 50$, $K_s = 20$, $C_d = 10$, $x_c = 0.25$ and $u = 1$. As predictable, when the gradient index is increased, the frequency ratio is increased.

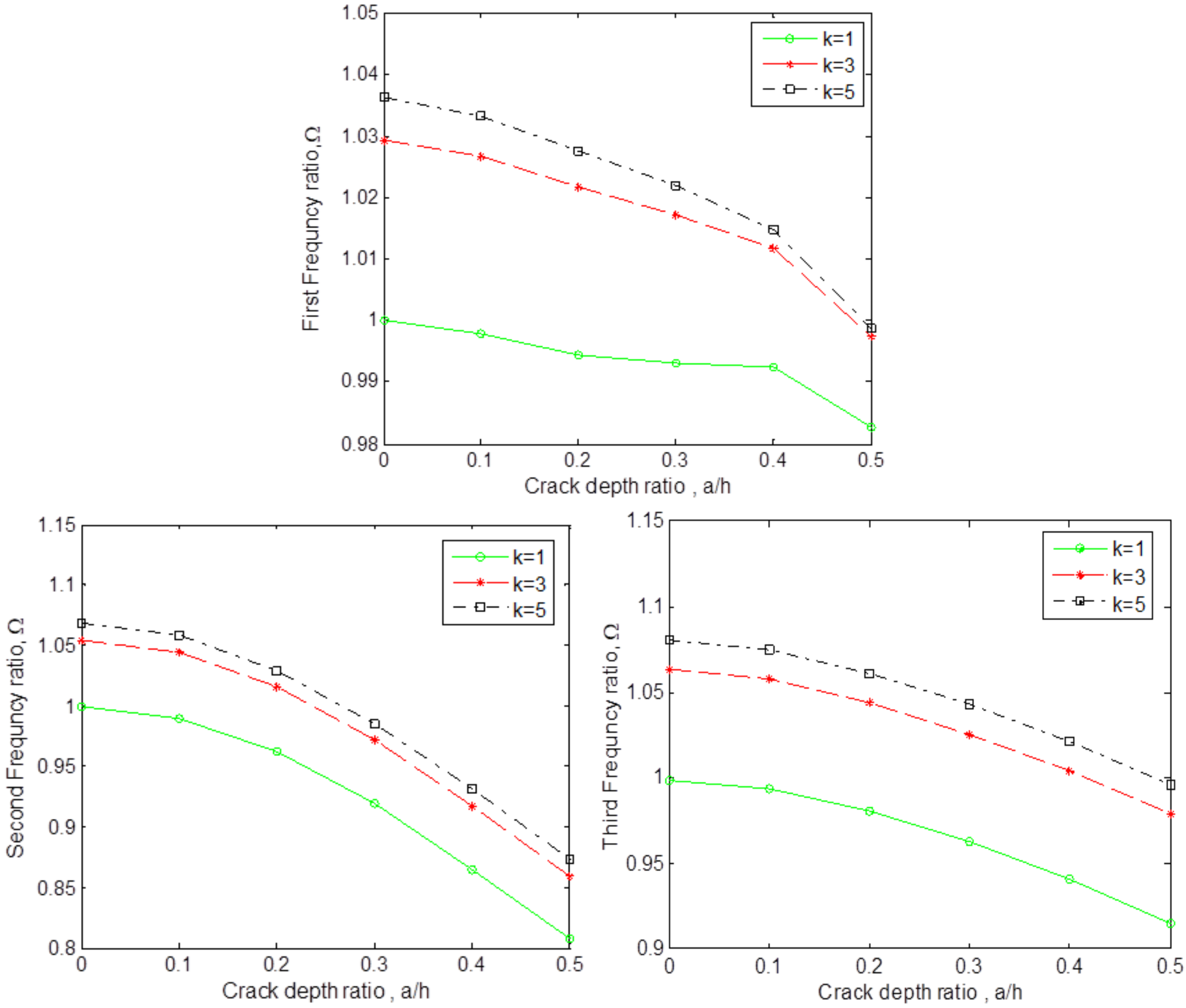

Figure 5. Effect of gradient index (k) on lowest three frequency ratio for (pinned-pinned) FG pipe.

Figure 6 shows the influence the gradient index (k) on first fundamental frequency for pinned cracked FG pipe versus crack location. Here, the results are presented for different gradient index, k = 0, k = 1, k = 3 and 5. In this case, $K_m = 50$, $K_s = 20$, $C_d = 10$, $a/h = 0.5$ and $u = 1$. Results indicate that the first frequency is increased as the gradient index is increased. As it can be seen, the location of the crack has a significant influence on the first frequency. Results indicate that the first frequency minimizes as $x_c = 0.5$ for pinned FG pipe. When the crack is in the midpoint of the pinned-pinned FG pipe, the first frequency is minimum.

6.3 Effect of flow velocity

This subsection shows the effect of the flow velocity on fundamental frequency of (P-P) FG pipe versus crack position. Figure 7 presents the infllunce of dimenssionless flow velocity (u) on dimensionless fundamental frequency for cracked FGM pipes at $K_m = 0.01$, $K_s = 0.01$, $C_d = 0.01$, $x_c = 0.5$ and

$a/h = 0.5$ for three boundary condition (pinned-pinned, clamped-clamped, clamped-free) boundary condition. Here, the results are presented for different dimensionless crack depth, k = 1, k = 3 and 5. In this case, $K_m = 50$, $K_s = 20$, $C_d = 10$, $x_c = 0.25$ and $u = 1$.. As it is seen from Figure 7, the first frequency is decreased as dimensionless flow velocity is increased.

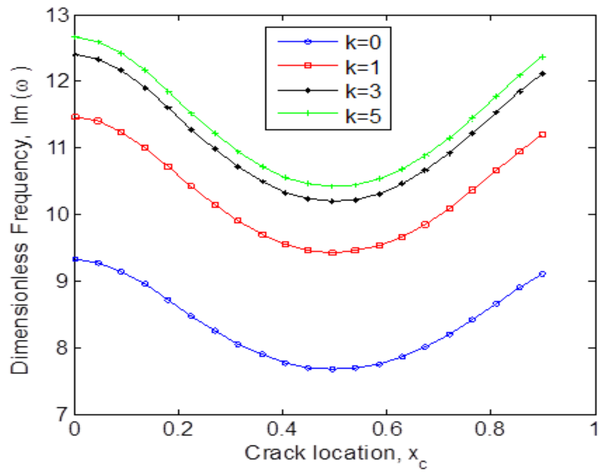

Figure 6. Effect of crack location on first dimensionless frequency with different gradient index for (P-P) boundary condition.

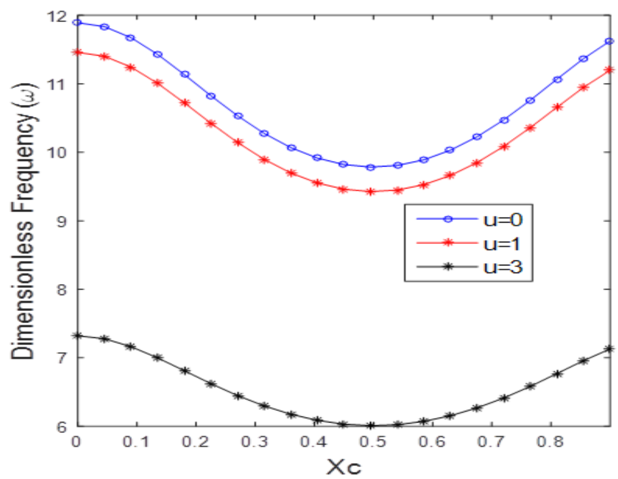

Figure 7. Effect of dimensionless flow velocity (u) on the dimensionless fundamental frequency for (P-P) boundary condition.

6.4 Effect of Viscoelastic Foundation parameter on cracked FGM pipe

This subsection demonstrated the effect of viscoelastic foundation parameter on natural frequency of simply supported end conditions of FG pipe with different dimensionless flow velocity. Figure 8 illustrates the effect of viscoelastic foundation parameter (K_m, K_s, and C_d) on the real and imaginary parts of system eigenvalues for pinned FG pipe conveying flow.

Figure 8(a) presents the first imaginary frequency and damping parts of fundamental eigenvalues for pinned FG pipe with different non-dimensional elastic modulus Km=0, 50 and 100. In this case, Ks =20, Cd=10, xc =0.25, a/h=0.5, and gradient index k =1. From this figure, it is seen that the vibration frequency increase as an increase in elastic modulus

On the other hand, the effect of shear modulus on the real and imaginary dimensionless frequency of the P-P FG pipe conveying flow is illustrated in Figure 8(b). Results are offered for different non-dimensional shear parameters, K_s = 0, K_s = 10 and K_s = 20. In this case, Km=50, Cd=10, xc =0.25, a/h=0.5, and gradient index k=1. The shear coefficient can be expected to have a function similar to the mass of the system, with an opposite effect (because of the negative signal). Thus, adding the shear coefficient is similar to removing some system mass. Note that, with increased shear modulus, the resonance frequencies are also increased. According to the above explanation for the increased shear coefficient, more mass is removed from the system and thus increased resonance frequencies

Figure 8(c) shows the effect of the damping factor on the real and imaginary dimensionless frequency of P-P FG pipe conveying flow. The results are offered for different values of the damping parameters, Cd=0, Cd = 10 and Cd = 20. In this case, Km=50, Ks=10, xc =0.25, a/h=0.5, and gradient index k=1. It was noted that with the increase of the damping factor, the system was damped, resulting in lower vibration frequencies for all modes.

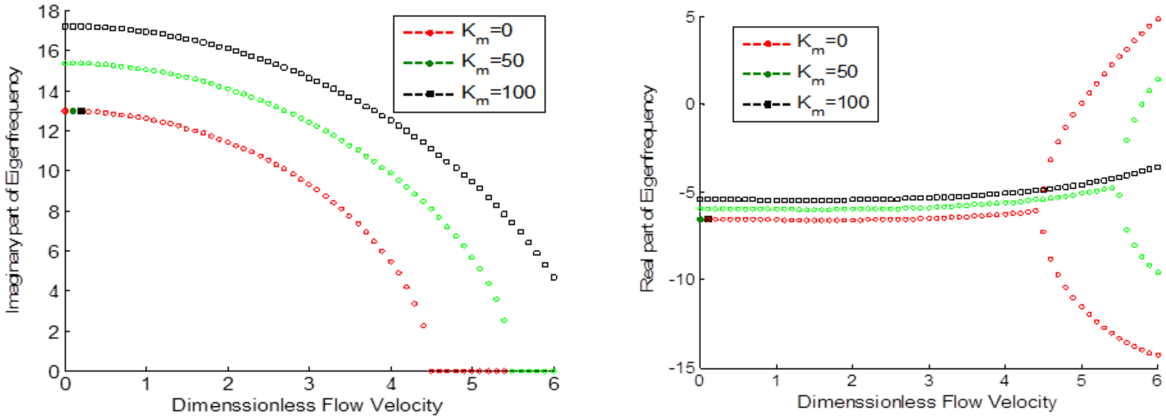

(a)

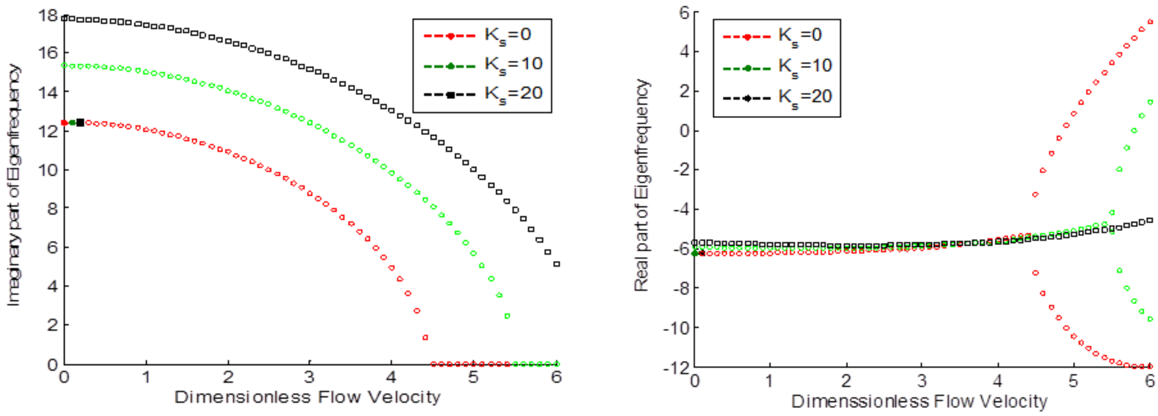

(b)

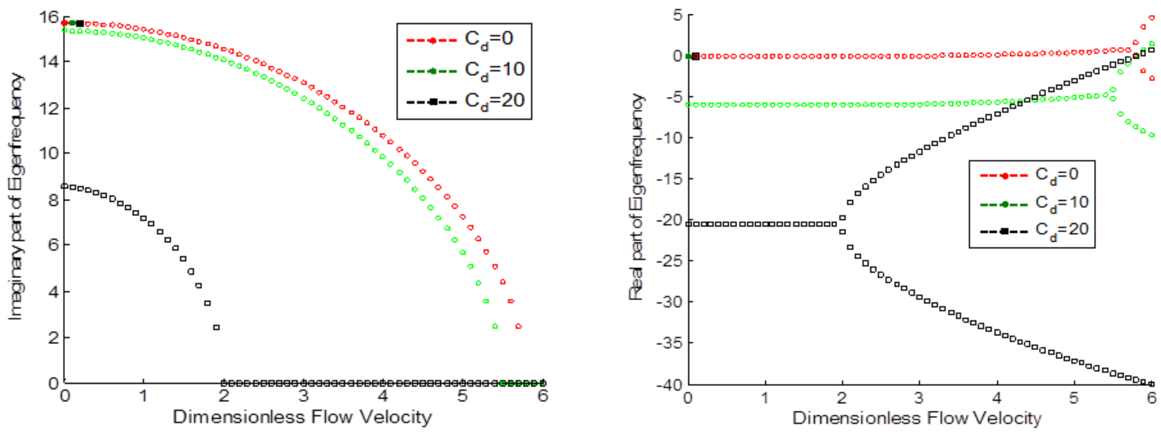

(c)

Figure 8. Viscoelastic foundation parameter effects on the real and imaginary dimensionless frequency of P-P FG pipe; (a) elastic foundation parameter, (b) shear parameter, and (c) damping parameter.

Figure 9 exhibits the lowest natural frequency as functions of the crack location with different elastic, shear, and damping parameter for viscoelastic foundation, respectively. The lowest natural frequency is sensitive to crack location and is decreased when the crack gets near to pipe midpoint. Also, the influence of the crack tends to be very small as the crack gets closer to the pipe ends. Also, it is seen from Figure 9, by increasing the elastic, and the shear parameter, the lowest natural frequency is increased, while by increasing the damping parameter, the lowest natural frequency is decreased.

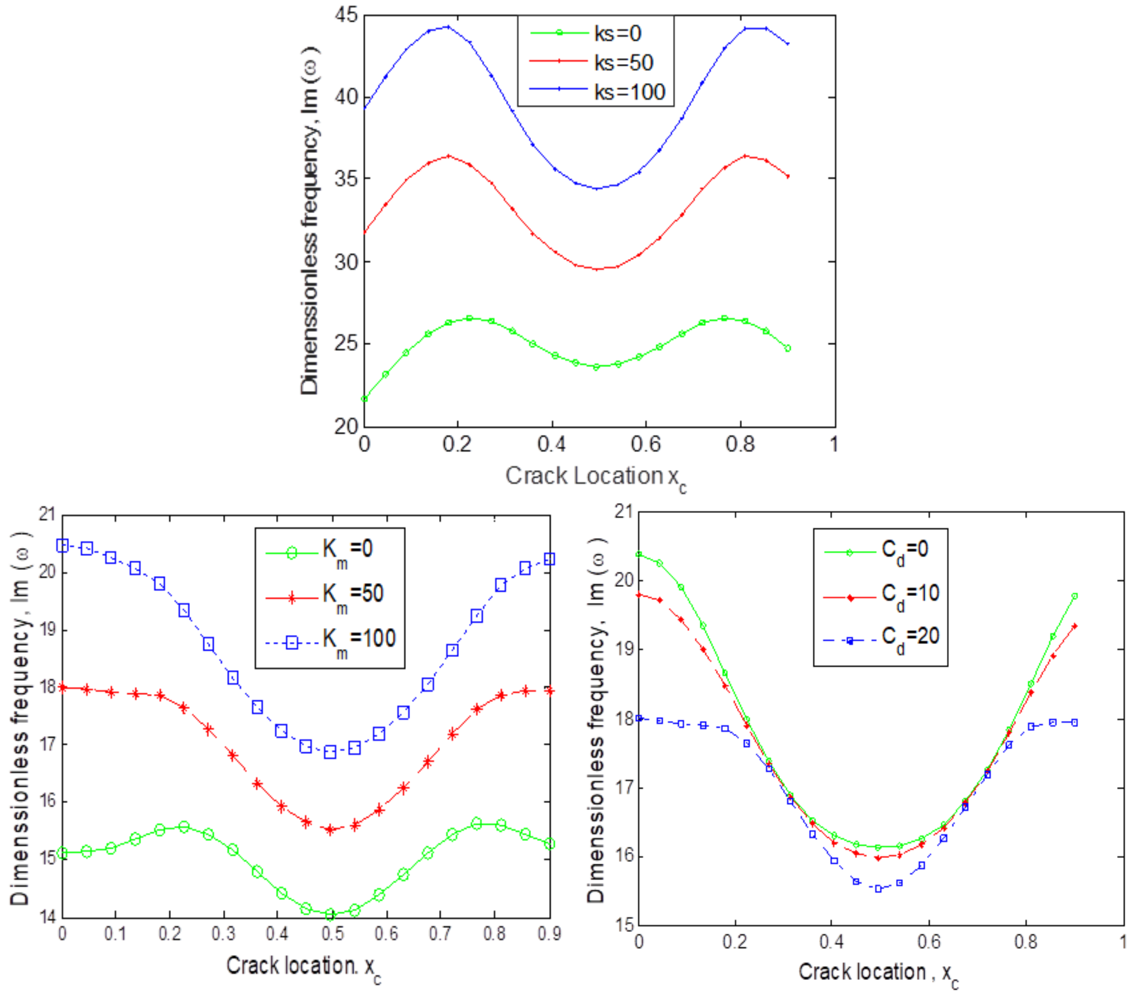

Figure 9. The first natural frequencies of the pinned FGM pipes conveying fluid as functions of crack location with different foundation parameter.

7. Conclusion

In this paper, the dynamic behavior of cracked FG pipe conveying flow on visco-elastic foundation is studied. Based on the Euler-Bernoulli beam theory, the vibration equation of the (simply supported) FG pipe is derived using Hamilton's principle. The properties of the material change constantly across the pipes thickness and depend on power law distribution. The vibration equations are discretized and solved numerically using the Galerkin's method. The local flexibility theory is utilized to simulate the crack, considering that the crack is a type I crack, and it is assumed that it is always in the open state during the vibration of the FG pipe. The spring is used to connect the pipe sections on both sides of the crack. In the numerical analysis section, the influence of different parameter on the vibration frequency of the cracked FG pipe is mainly discussed in detail. The numerical results show:

1. As the gradient index increases, the vibration frequency of the FGM flow pipe and the critical velocity of the (pinned-pinned) boundary will increase. In this way, we can improve the vibration and stability characteristics of the flow pipe by adjusting the gradient distribution of the FGM pipe material.
2. The frequency is decreased if the crack size is increased. For example, the pipe with crack position is 0.540 from length, the first nondimensional natural frequency for uncracked FG pipe is 18.005451and

for FG pipe with 0.3, and 0.5 crack depth ratio is 17.4512 and 16.0663 respectively, i.e. the reduction percent is 3.35% and 10.76% respectively.

3. With the increasing of crack depth, the fundamental natural frequency decreases (i.e. the crack depth tends to decrease the bending stiffness of the FG pipe conveying).
4. As the crack position increased, the fundamental natural frequency decreases as approaching the center of the pipe which belongs to the increase of deflection at the middle of the pipe.
5. With increasing of visco-elastic foundations (k_m, k_s, C), the cracked FG pipe is more difficult to show divergence stability
6. As the flow velocity increases, the vibration frequency of cracked FG pipe conveying fluid decreases. For example, the first nondimensional natural frequencies for cracked FG pipe with different nondimensional flow velocity (u=0, 2, 4) are (16.3787, 15.4048, and 12.2317 respectively) i.e. the non-dimensional frequency decreases by 5.94% and 25.3% respectively.

References

[1] Païdoussis, M. P., & Li, G. X. (1993). Pipes conveying fluid: a model dynamical problem. Journal of Fluids and Structures, 7(2), 137-204

[2] Mahjoob, M., Shahsavari, A., and Marzban, A. (2007). A Vibration-Based Damage Detection Method for Pipes Conveying Fluid. In 48th AIAA/ASME/ASCE/AHS/ASC Structures, Structural Dynamics, and Materials Conference (p. 2351).

[3] Son, I. S., Yoon, H. I., Lee, S. P., and Kim, D. J. (2010). Effects of tip mass on stability of rotating cantilever pipe conveying fluid with crack. International Journal of Modern Physics B, 24(15n16), 2609-2614.

[4] Kwan, H. D., Son, I. S., and Lee, S. C. (2012). Stability of Elastically Restrained Valve-pipe System with Crack. International Journal of Modern Physics: Conference Series, Vol. 6, pp. 373-378. DOI: 10.1142/S2010194512003467

[5] Sheng, Y. Z., Guo, C. Q., and Hong, W. B. (2015). Stability of Cracked Fluid-Conveying Pipeline on Elastic Foundation under Distributed Follower Forces. Advanced Materials Research Vols. 1065-1069, pp. 2076-2079, doi:10.4028/www.scientific.net/AMR.1065-1069.2076

[6] Eslami, G., Maleki, V. A., and Rezaee, M. (2016). Effect of open crack on vibration behavior of a fluid-conveying pipe embedded in a visco-elastic medium. Latin American Journal of Solids and Structures, 13(1), 136-154.

[7] Muhsin J. Jweeg, E. Q. Hussein, and K. I. Mohammed (2017) 'Effects of Cracks on the Frequency Response of a Simply Supported Pipe Conveying Fluid' International Journal of Mechanical & Mechatronics Engineering IJMME-IJENS, Vol. 17, 05.

[8] Sheng G.G., and X. Wang (2008) "Thermomechanical vibration analysis of a functionally graded shell with flowing fluid" European Journal of Mechanics A/Solids, 27, 1075-1087.

[9] Hosseini, M., and Fazelzadeh, S. A. (2011). Thermomechanical stability analysis of functionally graded thin-walled cantilever pipe with flowing fluid subjected to axial load. International Journal of Structural Stability and Dynamics, 11(03), 513-534.

[10] Liang, F., Yang, X. D., Bao, R. D., and Zhang, W. (2016). Frequency analysis of functionally graded curved pipes conveying fluid. Advances in Materials Science and Engineering, 2016.

[11] ZHU, C. G., and Si-Peng, X. U. (2016). Nonlinear Free Vibration Analysis of Fluid Conveying FG Tube via Energy Balance Method. International Conference on Applied Mechanics, Mechanical and Materials Engineering (AMMME 2016).

[12] Deng, J., Liu, Y., Zhang, Z., and Liu, W. (2017). Dynamic behaviors of multi-span viscoelastic functionally graded material pipe conveying fluid. Proceedings of the Institution of Mechanical Engineers, Part C: Journal of Mechanical Engineering Science, 231(17), 3181-3192.

[13] Tang, Y., and Yang, T. (2018). Post-buckling behavior and nonlinear vibration analysis of a fluid-conveying pipe composed of functionally graded material. Composite Structures, 185, 393-400.

[14] Wang, Z. M., and Liu, Y. Z. (2016). Transverse vibration of pipe conveying fluid made of functionally graded materials using a symplectic method. Nuclear Engineering and Design, 298, 149-159.

[15] Cao M., Xu W., Ostachowicz W., Su Z. Damage identification for beams in noisy conditions based on Teager energy operator-wavelet transform modal curvature. Journal of Sound and Vibration, Vol. 333, Issue 6, 2014, p. 1543-1553.

[16] Dimarogonas, A. D., and Paipetis, S. A. Analytical methods in rotor dynamics, 1983. App. Sc. Publishers, London.
[17] Yu, Z., Zhang, L., Hu, J., and Hu, J. (2016). Damage modeling and simulation of vibrating pipe with part-through circumferential crack. Journal of Vibroengineering, 18(4).
[18] Dimarogonas, A. D., and Papadopoulos, C. A. (1983). Vibration of cracked shafts in bending. Journal of sound and vibration, 91(4), 583-593.
[19] Fernandez-Saez, J., Rubio, L., and Navarro, C. (1999). Approximate calculation of the fundamental frequency for bending vibrations of cracked beams. Journal of Sound and Vibration, 225(2), 345-352.

